

Asymmetrical Load Mitigation of Wind Turbine Pitch Actuator Faults using Unknown Input-based Fault-tolerant Control

Yanhua Liu* Ron J. Patton* Shuo Shi*

* *Department of Engineering, University of Hull, Cottingham Road, Hull, HU6 7RX, UK (e-mail: Y.Liu@hull.ac.uk, r.j.patton@hull.ac.uk, S.Shi@2016.hull.ac.uk).*

Abstract: Offshore wind turbines suffer from asymmetrical blade loading, resulting in enhanced structural fatigue. Individual pitch control (IPC) is an effective method to achieve blade load mitigation, accompanied by enhancing the pitch movements and thus increased the probability of pitch actuator faults. The occurrence of faults will deteriorate the IPC load mitigation performance, which requires fault-tolerant control (FTC). IPC is itself analogous to the FTC problem because the action of rotor bending can be considered as a fault effect. Therefore, the work thus proposes a “co-design” strategy, constituting a combination of IPC-based asymmetrical load mitigation combined with FTC acting at the pitch system level. The FTC uses the well-known fault estimation and compensation strategy. A Proportional-Integral PI-based IPC strategy for blade mitigation is proposed in which the robust fault estimation is achieved using a robust unknown input observer (UIO). The performance of two pitch controllers (baseline pitch controller, PI-based IPC) are compared in the presence of pitch actuator faults (including low pressure & loss of effectiveness). The effectiveness of the proposed strategy is verified on the 5MW NREL wind turbine system.

Keywords: Individual pitch control, unbalanced load mitigation, pitch actuator faults, unknown input observer.

1. INTRODUCTION

Nowadays, the numbers of offshore wind turbines (WTs) are increasing to meet the growing energy demand for carbon-free energy. However, offshore WTs face two major challenges in the region 3 operation (above the rated wind speed). Firstly, unexpected WT component faults will lead to costly repairs and even months of turbine unavailability. Thus, this will increase the operation and maintenance (O&M) costs and enhance the levelized cost of energy. Especially, the pitch systems contribute approximately 22% of the annual turbine downtime just after the electrical subsystem (Wilkinson et al., 2010). Moreover, larger rotor blades and higher towers have resulted in enhanced asymmetrical blade loading due to wind turbulence, gravity, tower shadow, yaw misalignment, etc.

Individual pitch control (IPC) is effective to achieve rotor load mitigation (Bossanyi, 2005), but it can suffer from undesirable effects of enhanced pitch movements. This leads to an increased likelihood of pitch actuator faults which will cause further asymmetry in blade loading. The scenario of asymmetrical load reduction is analogous to the fault-tolerant control (FTC) because the action of rotor bending (caused by wind loading) can itself be considered as a fault effect. A fault acting in a system is an unwanted effect causing a performance deterioration and this is precisely what happens with rotor blade bending. It is

interesting to consider “fault effects” acting in the pitch actuation and rotor blade systems i.e. actuator faults and bending moment effects. The bending moment changes are effectively component faults acting in the rotor system.

Hence, it is important to jointly optimise the requirement for asymmetrical load mitigation whilst restricting control demands for large pitch variations. The multi-objectives arising in the FTC and load mitigation problems can thus be viewed as a “co-design” scheme, in which fault estimation (FE) based FTC to compensate the undesirable effect that pitch actuator faults have on the IPC system. This strategy aims to enhance the robustness and reliability of the pitch control system, thereby sustaining the load mitigation performance in a fault tolerant system.

Nonetheless, the research involving IPC with FTC in the presence of faults (referred to as “fault-tolerant individual pitch control”) is rarely considered. A fault diagnosis and accommodation technique for enabling or disabling the IPC according to the fault detection result of the azimuth angle sensor is proposed by (Odgaard et al., 2015). Root bending sensor faults can be detected online through the model-based estimation of first-harmonic blade load signal with the wind data from LiDAR system applied to the IPC system (Stotsky, 2014). These two sensors (i.e. azimuth angle sensor and blade root load sensor) provide important information for good IPC system performance. However, the 3 pitch actuators may have faulty components, i.e. the

actuators must also be monitored online. A fault detection and diagnosis (FDD) and automatic signal correction algorithm for a pitch actuator fault within an IPC is proposed in (Badihi and Zhang, 2018) which focuses on one hydraulic oil leak fault (leading to pressure drop). However, it uses an FDI-based FTC which is complex to implement in a real system since the uncertainty in detection involves a detection delay combined with a delay in switching to a healthy redundant control system. The main problem is that the WT rotor has no hardware redundancy, so this FDI-based FTC is impossible to use without an analytical scheme for generating redundant measurements. As an alternative to residual-based FDI an estimation strategy (i.e. FE) can be used that estimates both the fault effects and the pitch system states.

The contributions of this paper focus on proposing a “co-design” framework to maintain the on-line unbalanced load reduction performance when pitch actuator faults occur using FE-based FTC for preventive maintenance. The remainder is organized as follows. Section 2 shows the pitch actuator fault modelling including the low pressure fault and loss of effectiveness. Furthermore, Section 3 explains the “co-design” strategy containing the combined PI-based IPC system and FE-based FTC scheme, where a robust unknown input observer (UIO) is proposed to achieve estimates of pitch actuator faults. Illustrative simulations are provided in Section 4. Finally, Section 5 provides a summary and prospects for future research.

2. PITCH ACTUATOR FAULT MODELLING

This paper focuses on the pitch system related faults, thus the pitch system modelling is provided. A hydraulic pitch actuator modelled as a closed-loop second-order system (Odgaard et al., 2009) is applied in the NREL 5MW WT model to enable the actuator FE signals to be generated. The three pitch systems are assumed to have the same dynamics in the fault-free case, as shown in (1). Due to the physical system constraints, pitch angles and rates are restricted to $[0,90]^\circ$ and $[-8,8]^\circ/s$ in the simulation.

$$\frac{\beta}{\beta_r} = \frac{w_{n_0}^2}{s^2 + 2\xi_0 w_{n_0} s + w_{n_0}^2} \quad (1)$$

where ξ_0 and w_{n_0} are the nominal damping ratio and natural frequency parameters. β and β_r are the pitch actuator output and rated pitch angles, respectively.

2.1 Pitch Actuator Initial Faults with Changing Dynamics

A hydraulic pitch oil leak fault can arise due to an oil seal failure or improper management of hydraulic fluids, resulting in low oil pressure. On its own this fault requires manual off-line maintenance. If the oil pressure becomes too low, the pitch system will fail in pitching the corresponding blade to the required position. The hydraulic leakage fault will lead to the pitch system with changed dynamics (ξ_0, w_{n_0}), causing slow pitching performance and unstable turbine outputs. It will lead to the pitch actuator stuck fault (i.e. seized blade movement), requiring repair during turbine shut-down (Naik, 2017). The faulty parameters can be modelled as convex combinations of $\xi_0 w_{n_0}$, $w_{n_0}^2$ and the fault level θ_f (Liu et al., 2018):

$$\begin{aligned} w_n^2 &= w_{n_0}^2 + (w_{n_f}^2 - w_{n_0}^2)\theta_f \\ \xi_f w_n &= \xi_0 w_{n_0} + (\xi_f w_{n_f} - \xi_0 w_{n_0})\theta_f \end{aligned} \quad (2)$$

where ξ_f and w_{n_f} denote the dynamic parameters in the faulty case. The parameter $\theta_f \in [0, 1]$ indicates the fault level, where the larger the θ_f is, the more severe the actuator fault is. The dynamic parameters $w_{n_0} = 11.11 \text{ rad/s}$, $\xi_0 = 0.6$, $w_{n_f} = 3.42 \text{ rad/s}$, $\xi_f = 0.9$.

From (2), the corresponding pitch actuator state-space model with initial faults f_a and unknown disturbance d and measurement noise d_s can be illustrated as (3), where D and D_s denote disturbance distribution and sensor noise distribution matrices, β_m is the system output.

$$\begin{aligned} \begin{bmatrix} \dot{\beta} \\ \ddot{\beta} \end{bmatrix} &= \begin{bmatrix} 0 & 1 \\ -w_{n_0}^2 & -2\xi_0 w_{n_0} \theta_f \end{bmatrix} \begin{bmatrix} \beta \\ \dot{\beta} \end{bmatrix} + \begin{bmatrix} 0 \\ w_{n_0}^2 \end{bmatrix} \beta_r \\ &+ \begin{bmatrix} 0 \\ w_{n_0}^2 \end{bmatrix} f_a + Dd \\ \beta_m &= [1 \quad 0] \begin{bmatrix} \beta \\ \dot{\beta} \end{bmatrix} + E_s d_s \\ f_a &= (1 - \frac{w_{n_f}^2}{w_{n_0}^2})(\beta - \beta_r)\theta_f + 2(\frac{\xi_0}{w_{n_0}} - \frac{\xi_f w_{n_f}}{w_{n_0}^2})\theta_f \dot{\beta} \end{aligned} \quad (3)$$

2.2 Pitch Actuator Loss of Effectiveness (LOSS)

Blade pitch actuators normally operate exactly (i.e. 100% effectiveness) as referenced by the pitch controller. However, the long-term operation of pitch actuators without proper maintenance will lead to changes in the pitch actuator dynamic response including unknown loss of effectiveness faults (Habibi et al., 2018). This partial loss of effectiveness fault (<100% effectiveness) means that the pitch actuators cannot fulfil the pitch angle references from the CPC and IPC system timely and accurately. This generic actuator fault is normally caused by aging internal components which leads to hydraulic leakage, clogging pumps or changed dynamic parameters. Hence, the performances of both the power regulation and blade load mitigation are degraded seriously.

$$\beta = \gamma * \frac{w_n^2}{s^2 + 2\xi w_n s + w_n^2} * \beta_r \quad (4)$$

where $\gamma \in [0, 1]$ denotes the effectiveness level, $\gamma = 1$ means the actuator is 100% effective, $\gamma = 0$ is the total loss. The corresponding pitch actuator state-space model:

$$\begin{aligned} \begin{bmatrix} \dot{\beta} \\ \ddot{\beta} \end{bmatrix} &= \begin{bmatrix} 0 & 1 \\ -w_{n_0}^2 & -2\xi_0 w_{n_0} \theta_f \end{bmatrix} \begin{bmatrix} \beta \\ \dot{\beta} \end{bmatrix} + \begin{bmatrix} 0 \\ w_{n_0}^2 \end{bmatrix} \beta_r \\ &+ \begin{bmatrix} 0 \\ w_{n_0}^2 \end{bmatrix} f_a + Dd \\ \beta_m &= [1 \quad 0] \begin{bmatrix} \beta \\ \dot{\beta} \end{bmatrix} + E_s d_s \\ f_a &= (\gamma - 1)\beta_r \end{aligned} \quad (5)$$

The open-loop performance of one pitch actuator system in various faulty cases are evaluated and shown in Fig. 1.

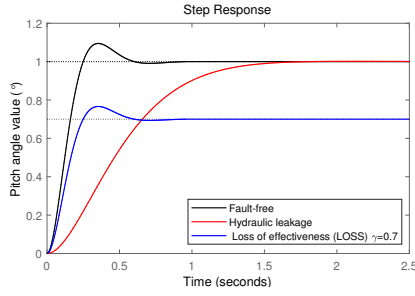


Fig. 1. Step response of one pitch actuator system

Therefore, the faulty pitch system based on (3) and (5) can be illustrated as:

$$\begin{aligned} \dot{x} &= Ax + Bu + F_a f_a + Dd \\ y &= Cx + E_s d_s \end{aligned} \quad (6)$$

where $x \in R^{n \times 1}$ and $u \in R^{m \times 1}$ represent the pitch system state matrix and control inputs, respectively. $y \in R^{p \times 1}$ denotes the system measurements. $d \in R^{l \times 1}$ means a combined effect of unknown disturbance and modelling uncertainty. $f_a \in R^{s \times 1}$, $F_a \in R^{n \times s}$ are the assumed actuator faults and fault distribution matrix. $E_s \in R^{p \times r}$ and $d_s \in R^{r \times 1}$ are the assumed measurement noise and sensor noise distribution matrix. The constant system matrices $A \in R^{n \times n}$, $B \in R^{n \times m}$, $D \in R^{n \times l}$, $C \in R^{p \times n}$ are known with $n = 6$, $m = 3$, $l = 6$, $p = 3$, $s = 3$, $r = 3$.

3. FTC-IPC SYSTEM DESIGN

The proposed ‘‘co-design’’ framework of FTC-IPC pitch system is shown in Fig.2, including (i) a baseline pitch controller (CPC) using gain-scheduled PI approach for generator power control (Jonkman et al., 2009), (ii) a PI-based IPC system for asymmetrical blade loading mitigation, (iii) a robust UIO system for pitch actuator fault estimation, and (iv) FE-based FTC for fault compensation.

3.1 PI-based IPC Design for Load Reduction

The ‘‘dissimilar redundancy’’ of the actuation in the IPC system is used to reduce three flapwise blade bending vibrations $M_{1,2,3}$ adjusting pitch angle $\beta_{1,2,3}$ individually. The Coleman transformation is adopted to map $M_{1,2,3}$ from the blade rotational system to the fixed hub reference (Bossanyi, 2005). After this, each blade load signal is converted to a collective mean component which is the

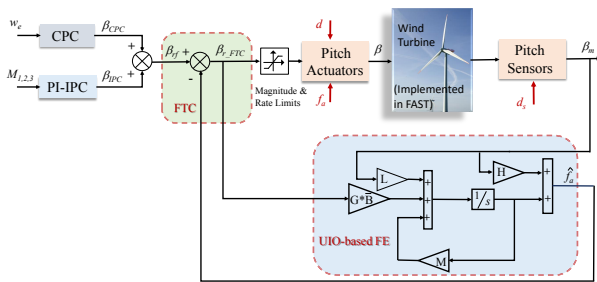


Fig. 2. Proposed ‘‘co-design’’ framework

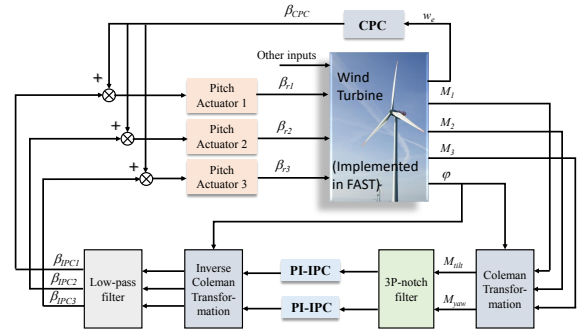


Fig. 3. Designed PI-based IPC system

same for three blades, a cosine and sine (referred to as yaw and tilt moments) component depending on $\varphi_{1,2,3}$. The significant unbalanced blade loading normally comes from the unsymmetrical wind inflow. Thus, the collective term is ignored for IPC design. The yaw and tilt loops can be treated as two independent channels and compensated by PI controller (Bossanyi, 2005). The inverse Coleman transformation is applied before adding up to the pitch angle from CPC. Reliable sensors (i.e. fibre optics, strain gauges) are required for the flapwise bending measurements.

The designed IPC system is shown in Fig.3, where the other inputs include wind dynamics and yaw angle etc. A notch filter is used to eliminate the 3P-harmonic loading peak signals after the Coleman transformation. A low-pass filter with cut-off frequency of 1.2Hz is used to smooth the control signals from the PI-based IPC, thus avoiding the high-frequency movements. The parameters of the two PI controllers are manually tuned to be the same by trial and error. More details about the designed PI-IPC controller can be found in the previous work (Liu et al., 2018).

3.2 FE-based FTC Design for Fault Compensation

UIO-based FE design To obtain the actuator fault estimation, the actuator fault f_a is augmented as a state and the first order derivative of the actuator faults \dot{f}_a is augmented as a disturbance, thus completing the augmented (state and fault) pitch system model as:

$$\begin{aligned} \dot{\bar{x}} &= \bar{A}\bar{x} + \bar{B}u + \bar{D}\bar{d} \\ y &= \bar{C}\bar{x} + E_s d_s \end{aligned} \quad (7)$$

$$\begin{aligned} \bar{A} &= \begin{bmatrix} A & F_a \\ \mathbf{0} & \mathbf{0} \end{bmatrix}, \bar{B} = \begin{bmatrix} B \\ \mathbf{0} \end{bmatrix}, \bar{D} = \begin{bmatrix} D & \mathbf{0} \\ \mathbf{0} & I \end{bmatrix}, \bar{C} = [C \ \mathbf{0}], \\ \bar{x} &= \begin{bmatrix} x \\ f_a \end{bmatrix}, \bar{d} = \begin{bmatrix} d \\ \dot{f}_a \end{bmatrix} \end{aligned}$$

where $\bar{x} \in R^{(n+s) \times 1}$, $\bar{d} \in R^{(l+s) \times 1}$ and $\bar{A} \in R^{(n+s) \times (n+s)}$, $\bar{B} \in R^{(n+s) \times m}$, $\bar{D} \in R^{(n+s) \times (l+s)}$, $\bar{C} \in R^{p \times (n+s)}$.

The following Assumptions and Lemmas form the basis for the robust UIO design:

Assumption 1. (A, C) is observable, (A, B) is controllable. The control matching condition is satisfied with $rank(B, F_a) = rank(B)$.

Assumption 2. f_a is differentiable and belongs to $\mathcal{L}_2[0, \infty)$.

Lemma 1. An error system with the following dynamics:

$$\dot{e} = Ce + E_s d_s$$

is asymptotically stable with H_∞ performance $\|G_{ed_s}\|_\infty < \lambda$, which can be illustrated as:

$$J = \int_0^\infty (e^T e - \lambda^2 d_s^T d_s) dt < 0 \quad (8)$$

By defining a Lyapunov function $V = e_x^T P e_x$ and P is a symmetric positive definite matrix. With assumed zero initial conditions, it holds that:

$$\begin{aligned} J &= \int_0^\infty (e^T e - \lambda^2 d_s^T d_s + \dot{V}) dt - \int_0^\infty \dot{V} dt \\ &= \int_0^\infty (e^T e - \lambda^2 d_s^T d_s + \dot{V}) dt - V(\infty) + V(0) \\ &\leq \int_0^\infty (e^T e - \lambda^2 d_s^T d_s + \dot{V}) dt \end{aligned}$$

One sufficient condition for (8) is illustrated as:

$$J_1 = e_y^T e_y - \lambda^2 w_d^T w_d + \dot{V} < 0$$

Lemma 2. A system $\dot{x} = Ax$ is termed \mathcal{D} -stable if all its eigenvalues η of the state matrix A lie within the region \mathcal{D} . Assume \mathcal{D} is a vertical strip region: $a_1 < \text{Re}(\eta_1) < b_1, a_1 < b_1 < 0$, the system $\dot{x} = Ax$ is \mathcal{D} -stable with the premise of existing a symmetric positive definite P_0 and satisfying the following LMI (Chilali and Gahinet, 1996), where \star represents the transpose of matrix elements in the symmetric position.

$$\begin{bmatrix} He(P_0 A + A^T P_0) - 2b_1 P_0 & 0 \\ \star & -He(P_0 A + A^T P_0) + 2a_1 P_0 \end{bmatrix} < 0$$

On satisfying the above Assumptions, the following UIO system (Chen et al., 1996) is proposed to estimate \bar{x} :

$$\begin{aligned} \dot{z} &= Mz + G\bar{B}u + Ly \\ \hat{x} &= z + Hy \end{aligned} \quad (9)$$

where $z \in R^{(n+s) \times 1}$ denotes the observer states, and $\hat{x} \in R^{(n+s) \times 1}$ is the estimate of \bar{x} . The designed matrices $M \in R^{(n+s) \times (n+s)}$, $G \in R^{(n+s) \times (n+s)}$, $L \in R^{(n+s) \times p}$ and $H \in R^{(n+s) \times p}$ are of appropriate dimensions.

The estimation error state is $e_x = \bar{x} - \hat{x}$, with dynamics:

$$\begin{aligned} \dot{e}_x &= \dot{\bar{x}} - \dot{\hat{x}} \\ &= (\Xi\bar{A} - L_1\bar{C})e_x + \Theta_1 z + \Theta_2 y + \Theta_3 u \\ &\quad + \Xi\bar{D}\bar{d} - L_1 E_s d_s - H E_s \dot{d}_s \end{aligned} \quad (10)$$

$$e_y = \bar{C}e_x + E_s d_s$$

$$\begin{aligned} \Xi &= I_{n+s} - H\bar{C}, L = L_1 + L_2, \Theta_1 = \Xi\bar{A} - L_1\bar{C} - M \\ \Theta_2 &= (\Xi\bar{A} - L_1\bar{C})H - L_2, \Theta_3 = (\Xi - G)\bar{B} \end{aligned} \quad (11)$$

To guarantee asymptotic stability of system (10), it is further assumed that the following conditions are satisfied:

$$M \text{ is Hurwitz, } \Theta_1 = 0, \Theta_2 = 0, \Xi - G = 0 \quad (12)$$

By satisfying (11)-(12), the error system (10) becomes:

$$\begin{aligned} \dot{e}_x &= (\Xi\bar{A} - L_1\bar{C})e_x + \Xi\bar{D}\bar{d} - L_1 E_s d_s - H E_s \dot{d}_s \\ e_y &= \bar{C}e_x + E_s d_s \end{aligned} \quad (13)$$

The term $\Xi\bar{D}\bar{d} - L_1 E_s d_s - H E_s \dot{d}_s$ indicates the effects of system disturbance and measurement noise acting on the UIO error dynamic (13). These uncertainties limit the

accuracy of the UIO system state and fault estimates. Hence, the augmented observer (9) is required to be both stable and a robust UIO system with e_x converging asymptotically to zero in finite time. This requires all the eigenvalues of M to be assigned to the left half complex plane. Here, the effects of uncertainties are attenuated using H_∞ optimization (Lan and Patton, 2016).

Theorem 1. If there exist a symmetric positive definite matrix $P \in R^{(n+s) \times (n+s)}$ and appropriate matrices $M_1 \in R^{(n+s) \times s}$ and $M_2 \in R^{(n+s) \times s}$, the error system (13) is robustly stable with H_∞ performance satisfying $\|G_{e_x \bar{d}}\|_\infty < \lambda$ for any disturbance $w_d \in \mathcal{L}_2(0, \infty)$ and a specific constant parameter λ . Thus one sufficient condition is:

$$\begin{bmatrix} \Delta_{11} & (P - M_1\bar{C})\bar{D} & -M_2 E_s + \bar{C}^T E_s & -M_1 E_s & \bar{C}^T \\ \star & -\lambda^2 I & 0 & 0 & 0 \\ \star & \star & E_s^T E_s - \lambda^2 I & 0 & 0 \\ \star & \star & \star & -\lambda^2 I & 0 \\ \star & \star & \star & \star & -I \end{bmatrix} < 0 \quad (14)$$

where $\Delta_{11} = He(P\bar{A} - M_1\bar{C}\bar{A} - M_2\bar{C})$, with $He(X) = X + X^T$. $M_1 = PH$, $M_2 = PL_1$. The disturbance matrix $w_d = [\bar{d} \ d_s \ \dot{d}_s]^T$. This theorem can be proved by *Lemma 1* and the Schur Complement Theorem (Boyd et al., 1994).

On satisfying the LMI (14), the availability of designed UIO with stable error dynamics is guaranteed. However, e_x will further affect the closed-loop system transient performance, which can be attenuated if the observer dynamics are designed to be much faster than the closed-loop system dynamics. Therefore, a pole placement constraint introduced in *Lemma 2* is used to place the eigenvalues of matrix M within a suitable vertical strip region.

Remark 1. The observer eigenvalues (13) can be placed to the vertical region $\mathcal{D} : a < \text{Re}(\eta) < b$ with given negative scalars a and b ($a < b < 0$), such that:

$$\begin{bmatrix} 2\Delta_{11} - 2bP & 0 \\ \star & -2\Delta_{11} + 2aP \end{bmatrix} < 0 \quad (15)$$

A positive constant λ together with negative parameters a, b are selected appropriately. By solving the LMIs (14) and (15), P, M_1, M_2 can be achieved. Furthermore, the matrices L_1 and H are obtained with $H = P^{-1}M_1, L_1 = P^{-1}M_2$. Thus M, G, H and L can be achieved subsequently with (11)-(12). Therefore, the actuator fault estimation \hat{f}_a can be achieved by the designed UIO system.

FTC design Given that the actuator fault is matched, the pitch actuator fault can be compensated directly using a straightforward strategy to achieve fault-tolerance, whereby the reconstructed faults are subtracted from the pitch control reference:

$$\beta_{r_FTC} = \beta_{rf} - \hat{f}_a \quad (16)$$

Moreover, \hat{f}_a is set to zero in the first 10s of the simulation to avoid feeding back the initial transients. After applying the correction (16), the pitch system with FTC is:

$$\begin{aligned} \dot{x} &= Ax + B(u - \hat{f}_a) + F_a f_a + Dd \\ y &= Cx \end{aligned} \quad (17)$$

4. SIMULATION RESULTS

The proposed “co-design” strategy is validated on the 5MW NREL FAST V8 wind turbine model (Jonkman et al., 2009). The stochastic and full-field turbulent wind speed input file is generated by the TurbSim simulator (Jonkman, 2009). The simulation is carried out at the above-rated wind speed of 1000s with an average wind speed at the hub-height of 18 m/s, a turbulence intensity of 13% and a vertical shear exponent of 0.2. Pitch actuator 1 is assumed to suffer from the hydraulic leakage fault during $t \in [300, 700]s$ and pitch actuator 2 suffers from the effectiveness loss fault with $\gamma = 0.7$ within $t \in [600, 1000]s$. The measurement noise d_s and unknown disturbance d are modelled as a zero mean white Gaussian noise with a variance value of $1.0e-7$ and $1.0e-6$, respectively. The LMIs (14) and (15) are solved with the *MATLAB*'s *LMI Control Toolbox* with $\lambda = 0.3, a = -10, b = -2$.

The standard deviations (STD) of three blade flap-wise bending moment, main-bearing tilt/yaw moment and generator power from 30s to 1000s avoiding the initial transit are compared in Table 1. The pitch travel ($\int_0^t |d\beta/dt| dt$, rad) is used to approximate the pitch actuator movements. STD describes the variations of considered parameters. Increases in STD and pitch travel denote performance degradation. PI-IPC refers to the system including both CPC and PI-based IPC. PI-IPC-f denotes the PI-IPC with pitch actuator faults. PI-IPC-F represents the PI-IPC-f with the corresponding FTC system implemented. Similar explanations follow for the other cases.

Table 1. The STD of Simulation Results

Parameters	CPC	CPC-f	CPC-F	PI-IPC	PI-IPC-f	PI-IPC-F
Gen-power (KW)	96.6	109.1	97.9	99.1	113.7	100.8
Flapwise 1 (KN-m)	1977.1	2150.0	1987.1	1439.6	1766.7	1486.8
Flapwise 2 (KN-m)	1973.5	2361.2	1979.0	1434.7	1703.0	1458.3
Flapwise 3 (KN-m)	1957.4	2142.9	1965.1	1418.4	1560.4	1430.6
Tilt (KN-m)	988.2	1499.9	987.6	701.8	1057.1	720.9
Yaw (KN-m)	850.8	1420.1	852.1	645.4	1000.4	670.8
Pitch travel 1 (rad)	7.9	8.7	11.4	37.4	37.5	41.5
Pitch travel 2 (rad)	7.7	7.5	13.2	37.4	34.7	37.3
Pitch travel 3 (rad)	7.7	8.5	7.8	37.0	39.6	37.0

The FE results of the considered pitch actuator faults in the PI-IPC case are illustrated in Fig. 4 and Fig. 5. The pitch fault estimates present a good match with the real fault value. This verifies that the proposed robust UIO can achieve accurate FE by decoupling the system uncertainties, measurement noise and pitch actuator faults.

Furthermore, the pitch references β_{r1} & β_{r2} and actual pitch actuator outputs β_1 & β_2 in the PI-based IPC fault-free case and faulty case are presented in Figs. 6-7. The pitch references β_{r1} & β_{r2} have been increased in the PI-IPC-f case to compensate the unimplemented pitch reference due to the pitch actuator faults, especially the effectiveness loss fault. Moreover, the pitch actuator outputs follow the real-time pitch references very well with designed FE-based FTC strategy. The generator power output, main-bearing tilt moment and blade flapwise bending moment 1 & 2 are shown in Figs. 8-9. The load reduction performance introduced by the PI-based IPC scheme and the generator power fluctuation have deteriorated with the pitch actuator faults considered. From Table 1, the proposed UIO-based FTC strategy works very well in both the CPC and PI-based IPC cases. This shows that

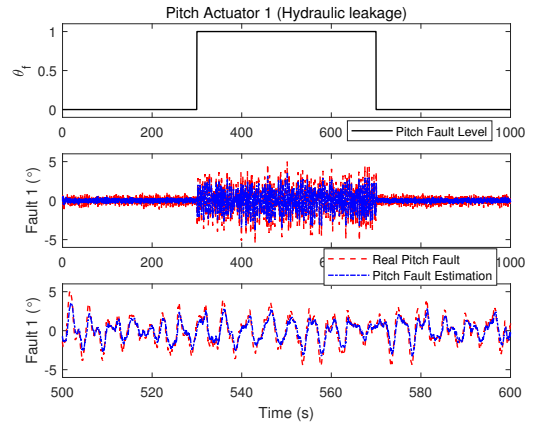


Fig. 4. Fault estimation of pitch system 1 in PI-IPC case

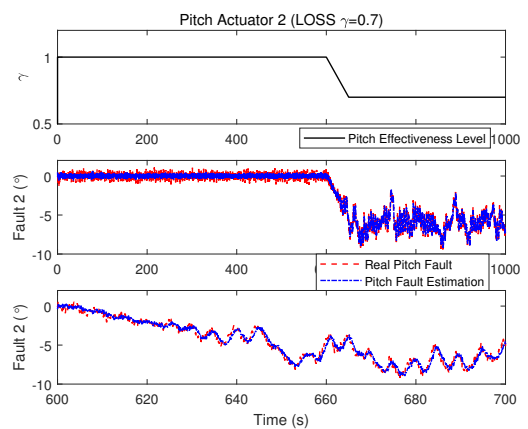


Fig. 5. Fault estimation of pitch system 2 in PI-IPC case

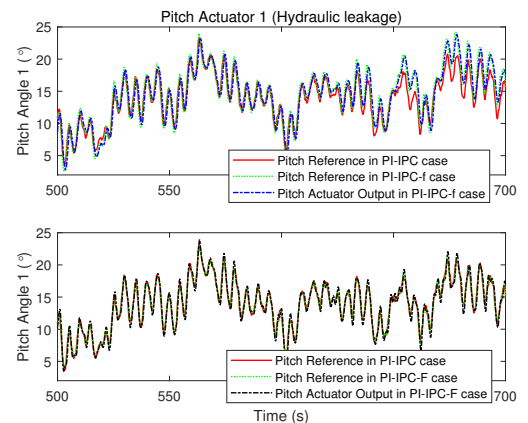


Fig. 6. Pitch reference 1 & actual pitch actuator output 1

the system performances including the generator power output and load mitigation property in the faulty case are recovered to a similar level compared with the fault-free case. In terms of pitch travel, it can be concluded that the pitch movements can be enhanced by the IPC system, the pitch faults and the introduced fault-tolerant scheme.

5. CONCLUSION

This paper proposes an IPC-based FTC “co-design” strategy for WT asymmetrical load mitigation with pitch actu-

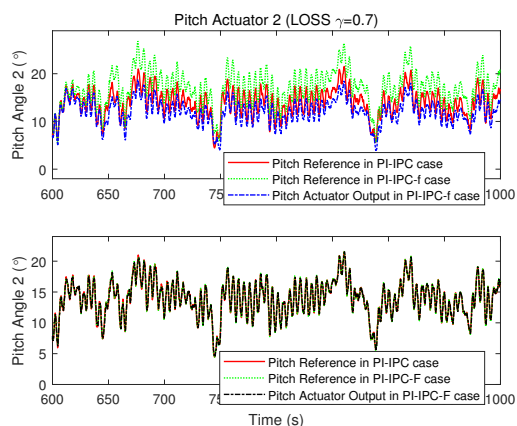


Fig. 7. Pitch reference 2 & actual pitch actuator output 2

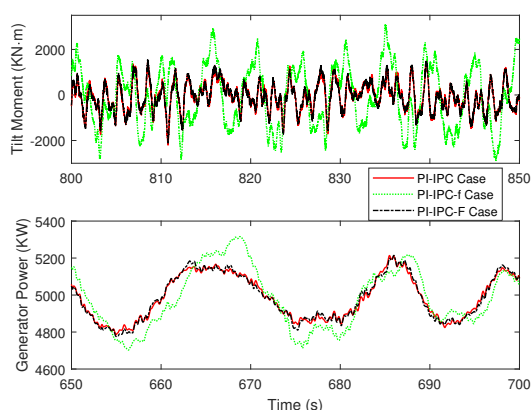


Fig. 8. Wind turbine power output and tilt moment

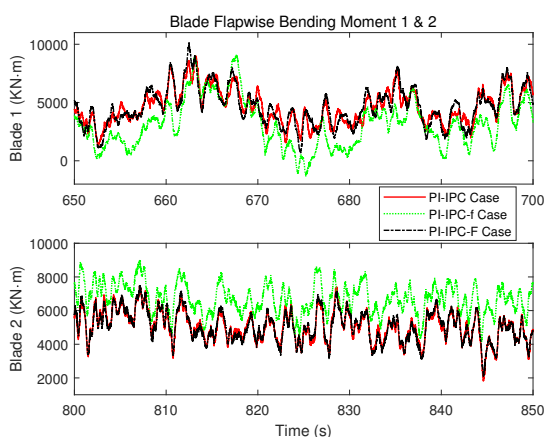


Fig. 9. Wind turbine flapwise bending performance

ator faults, thus sustaining the load balancing performance in a fault-tolerant system. Two types of pitch actuator faults including hydraulic leakage and loss of effectiveness are estimated and compensated by a robust UIO-based FTC system considering system uncertainty and measurement noise within baseline pitch system or PI-based IPC system. The simulation results verify the effectiveness and robustness of the proposed strategy. This strategy provides good load reduction and fault-tolerance feature in an effective way without major changes in pitch actuator design. This work will enhance the O&M procedure and OWT

sustainability. Further work will include studying the pitch actuator bias fault and the closed-loop performance using the proposed strategy during a start-up condition.

6. ACKNOWLEDGEMENT

The authors thank the China Scholarship Council and the Hull-China Scholarship for PhD funding support for Yanhua Liu. Thanks are also expressed to the UK EPSRC for funding support in the project “A New Partnership in Offshore Wind” through grant ref EP/R004900/1.

REFERENCES

- Badihi, H. and Zhang, Y. (2018). Fault-tolerant individual pitch control of a wind turbine with actuator faults. *IFAC-PapersOnLine*, 51(24), 1133–1140.
- Bossanyi, E. (2005). Further load reductions with individual pitch control. *Wind Energy*, 8(4), 481–485.
- Boyd, S., El Ghaoui, L., Feron, E., and Balakrishnan, V. (1994). *Linear matrix inequalities in system and control theory*, volume 15. Siam.
- Chen, J., Patton, R.J., and Zhang, H.Y. (1996). Design of unknown input observers and robust fault detection filters. *International Journal of control*, 63(1), 85–105.
- Chilali, M. and Gahinet, P. (1996). H/sub/spl inf/in/design with pole placement constraints: an LMI approach. *IEEE Transactions on automatic control*, 41(3), 358–367.
- Habibi, H., Nohooji, H.R., and Howard, I. (2018). Adaptive PID control of wind turbines for power regulation with unknown control direction and actuator faults. *IEEE Access*, 6, 37464–37479.
- Jonkman, B.J. (2009). Turbsim user’s guide: Version 1.50.
- Jonkman, J., Butterfield, S., Musial, W., and Scott, G. (2009). Definition of a 5-MW reference wind turbine for offshore system development. *Technical Report No. NREL/TP-500-38060*.
- Lan, J. and Patton, R.J. (2016). A new strategy for integration of fault estimation within fault-tolerant control. *Automatica*, 69, 48–59.
- Liu, Y., Patton, R.J., and Lan, J. (2018). Fault-tolerant individual pitch control using adaptive sliding mode observer. In *IFAC Safeprocess*, volume 51, 1127–1132. Warsaw, Poland.
- Naik, G.R. (2017). *Advances in Principal Component Analysis: Research and Development*. Springer Singapore. <https://doi.org/10.1007/978-981-10-6704-4>.
- Odgaard, P.F., Sánchez, H., Escobet, T., and Puig, V. (2015). Fault diagnosis and fault tolerant control with application on a wind turbine low speed shaft encoder. *IFAC-PapersOnLine*, 48(21), 1357–1362.
- Odgaard, P.F., Stoustrup, J., and Kinnaert, M. (2009). Fault tolerant control of wind turbines—a benchmark model. *IFAC Proceedings Volumes*, 42(8), 155–160.
- Stotsky, A. (2014). Blade root moment sensor failure detection based on multibeam LiDAR for fault-tolerant individual pitch control of wind turbines. *Energy Science & Engineering*, 2(3), 107–115.
- Wilkinson, M., Hendriks, B., Spinato, F., Harman, K., and Gomez, e. (2010). Methodology and results of the reliawind reliability field study. In *European Wind Energy Conference and Exhibition*, volume 3, 1984–2004. Warsaw, April.